Reduced-complexity air quality intervention modelling over China: development of the InMAPv1.6.1-China and comparison with the CMAQv5.2 model

Ruili Wu[1,2], Christopher W. Tessum[3], Yang Zhang[4], Chaopeng Hong[5], Yixuan Zheng[6], Qiang Zhang[1],Xinyin Qin[1], Shigan Liu[1]

[1]Ministry of Education Key Laboratory for Earth System Modelling, Department of Earth System Science, Tsinghua University, Beijing 100084, China

[2]State Environmental Protection Key Laboratory of Quality Control in Environmental Monitoring, China National Environmental Monitoring Centro, Beijing 100012, China

[3]Department of Civil and Environmental Engineering, University of Illinois at Urbana-Champaign, Urbana, Illinois 61801, United States

[4]Department of Civil and Environmental Engineering, Northeastern University, Boston, Massachusetts 02115, United States

[5]Department of Earth System Science, University of California, Irvine, California 92602, United States

[6]Center of Air Quality Simulation and System Analysis, Chinese Academy of Environmental Planning, Beijing 100012, China

Correspondence to: Ruili Wu (wurl15@tsinghua.org.cn or wurl@cnemc.cn)

Abstract. This paper presents the first development and evaluation of the reduced-complexity air quality model for China. In this study, a reduced-complexity air quality intervention model over China (InMAP-China) is developed by linking a regional air quality model, a reduced-complexity air quality model, an emission inventory database for China, and a health impact assessment model to rapidly estimate the air quality and health impacts of emission sources in China. The modelling system is applied over mainland China for 2017 under various emission scenarios. A comprehensive model evaluation is conducted by comparison against conventional CMAQ simulations and ground-based observations. We found that InMAP-China satisfactorily predicted total $PM_{2.5}$ concentrations in terms of statistical performance. Compared with the observed $PM_{2.5}$ concentrations, the mean bias (MB), normalized mean bias (NMB), and correlations of the total $PM_{2.5}$ concentrations are -8.1 μg/m^3, -18%, and 0.6, respectively. The statistical performance is considered to be satisfactory for a reduced-complexity air quality model and remains consistent with that evaluated in the United States. The underestimation of total $PM_{2.5}$ concentrations was mainly caused by its composition, primary $PM_{2.5}$. In terms of the ability to quantify source contributions of $PM_{2.5}$ concentrations, InMAP-China presents similar results in comparison with

those based on the CMAQ model, the difference is mainly caused by the different treatment of secondary inorganic aerosols in the two models. Focusing on the health impacts, the annual $PM_{2.5}$-related premature mortality estimated using InMAP-China in 2017 was 1.92 million, which was 25 ten thousand deaths lower than that estimated based on CMAQ simulations as a result of underestimation of $PM_{2.5}$ concentrations. This work presents a version of the reduced-complexity air quality model over China, provides a powerful tool to rapidly assess the air quality and health impacts associated with control policy, and to quantify the source contribution attributable to many emission sources.

1 Introduction

With rapid urbanization and industrialization, fine particulate matter pollution less than 2.5 μm in diameter ($PM_{2.5}$) has become a major environmental issue in China. High $PM_{2.5}$ concentrations can be observed over eastern China from satellite observations (Xiao et al., 2020) and the $PM_{2.5}$ concentrations have been largely decreased since 2013 due to the effective control measures taken by Chinese governments (Zhao et al., 2021). $PM_{2.5}$ can affect air quality, ecosystems, and climate change and damage human health through short-term or long-term exposure. The Global Burden of Disease study reported that 1.1 million premature deaths were caused by long-term $PM_{2.5}$ exposure over China in 2015 (Cohen et al., 2017).

State-of-the-science three-dimensional air quality models (AQMs) have been widely used in China as tools to simulate regional $PM_{2.5}$ concentrations, quantify the contributions to total $PM_{2.5}$ concentrations resulting from emission sources and assess the benefits associated with control measures (Chang et al.; 2019, Li et al., 2015; Zhang et al., 2015; Zhang et al., 2019). The Weather Research and Forecasting model-Community Multiscale Air Quality Modelling System (WRF-CMAQ) (Appel et al., 2017; Chang et al., 2019), the Weather Research and Forecasting model coupled with Chemistry (WRF-Chem) (Reddington et al., 2019), the Weather Research and Forecasting model-Comprehensive Air Quality Model Extension (WRF-CAMx) (Li et al., 2015), and the Global Adjoint model of Atmospheric Chemistry (GEOS-Chem Adjoint) (Zhang et al., 2015) were frequently used in previous studies. To conduct a series of simulations for multiple scenarios or quantify the separate contributions attributable to multiple sources, large computational resources and run time are required while utilizing conventional AQMs. To address these challenges and to improve the availability and accessibility of air quality modelling, a number of reduced-complexity models have been developed by the air quality research

community. The three representative reduced-complexity air quality models frequently used are the Estimating Air Pollution Social Impacts Using Regression (EASIUR) model (Heo et al., 2016; Heo et al., 2017), the updated Air Pollution Emission Experiments and Policy (APEEP2) model (Muller et al., 2007; Muller et al., 2011) and the Intervention for Air Pollution model (InMAP) (Tessum et al., 2017). A recent study compares three reduced-complexity models, EASIUR, APEEP2, and InMAP, and the results indicate that these three models are consistent in their assessment of the marginal social cost at the county level (Gilmore et al., 2019). Reduced-complexity air quality models are less computationally intensive and easier to use. However, it is not available for China. Therefore, it is essential to develop a reduced-complexity air quality model over China to quickly predict $PM_{2.5}$ concentrations and the associated health impacts of emission sources.

The reduced-complexity intervention model for air pollution, InMAP, was developed by Tessum et al. (Tessum et al., 2017) to rapidly assess the air pollution, health, and economic impacts resulting from marginal changes in air pollutant emissions. Compared with conventional air quality models, InMAP has the advantage of time efficient, can predict annual-average $PM_{2.5}$ concentrations within few hours but with a modest reduction in accuracy compared with CTMs. InMAP reduces the running time by simplifying the physical and chemical process. InMAP has been used to assess marginal health damage of location-specific emission sources (Goodkind et al., 2019), to quantify the health impacts of individual coal-fired power plants in the United States (Thind et al., 2019) and to estimate the health benefits of control policies considering specific locations (Sergi et al., 2020). However, to date, a version of the reduced-complexity air quality intervention model over China is absent.

In this work, based on the source code of the version 1.6.1 of InMAP model，a reduced-complexity air quality intervention model over China (InMAP-China) is developed to rapidly predict the air quality and estimate the health impacts of emission sources in China. The total consumed time for a simulation for the year 2017 using the InMAP-China established in this study is approximately an hour with a single CPU of 24 nodes. Therefore, it is convenient when conducting multiple simulations of $PM_{2.5}$ concentrations due to air pollutants emissions in 2017. The modelling system is applied over mainland China for 2017 under various emission scenarios to examine model performance. Comparisons against conventional air quality models and surface observations are performed in this study. The model applicability and limitations are also declared.

The paper is organized as follows: Section 2.1 presents the components of InMAP-China including the interface development between WRF-CMAQ and InMAP to generate parameters of the base

atmospheric state, the preprocessed process of emission input data and the exposure-response functions employed in this model. Section 2.2 introduces the evaluation protocol, including the statistical variables adopted and the simulation design in this study. Section 3 presents the evaluation of InMAP-China's predictions of $PM_{2.5}$ air quality and $PM_{2.5}$-related health impacts in several simulations. Section 4 summarizes the conclusions and limitations of this study.

2 Description of InMAP-China model

2.1 Model components and configurations

The reduced-complexity intervention model for air pollution, InMAP, was developed by Tessum et al. (Tessum et al., 2017) to rapidly assess the air pollution, health, and economic impacts resulting from marginal changes in air pollutant emissions. The model has been widely used in studies (Sergi et al., 2020; Thind et al., 2019; Goodkind et al., 2019; Dimanchevi et al., 2019) focusing on $PM_{2.5}$ pollution and health, economic impacts resulting from emission sources in the United States. In this model, the continuous equation of atmospheric pollutants is solved at an annual scale, and the run time can be reduced. The parameters used to represent physical and chemical processes for simplified simulation are calculated prior to using CTM output data. $PM_{2.5}$ air quality and $PM_{2.5}$-related premature mortality are predicted and output in the InMAP model.

In this work, a Chinese version of the reduced-complexity air quality intervention model InMAP-China is developed for the purpose of rapidly estimating the $PM_{2.5}$ concentration and associated health impacts of emission sources. Figure 1 shows the model framework. Based on the source code of the InMAP model, three-step development work is conducted to establish InMAP-China. First, we develop a preprocessed interface to calculate physical and chemical process parameters using the WRF-CMAQ output variables to support the simplified simulation in InMAP-China. Second, air pollutant emission data are preprocessed to an appropriate format for the InMAP-China simulation. Third, the exposure-response function of the GEMM model is employed in InMAP-China and replaces the original default function to assess $PM_{2.5}$-related health impacts.

Table 1 presents the basic configurations of InMAP-China. The simulation domain is over East Asia and covers mainland China. The spatial resolution is 36 km. Fourteen vertical layers are used in InMAP-China, ranging from the surface layer to the top level of the tropospheric layer.

2.1.1 Parameter interface development for simplified simulation in InMAP-China

We develop a preprocessed interface to calculate physical and chemical process parameters using WRF-CMAQ output variables for simplified simulation in InMAP-China based on the Environmental Protection Agency's (EPA) work (Baker et al., 2020). Two NETCDF files containing the key parameters for simplified simulation are generated by using the parameter interface developed here, one is at 36km resolution across entire mainland of China and another is at 4km resolution over the BTH region. The main step of the preprocessed interface includes meteorological and chemical variable extraction and merging, unit conversion, vertical layer mapping, physical and chemical process parameter calculation and average processing. The hourly chemical and meteorological variable outputs from the WRF-CMAQ modelling system are converted into annual-average physical and chemical process parameters required for simplified simulation.

A NETCDF file containing the three-dimensional annually averaged parameters to characterize atmospheric advection, dispersion, mixing, chemical reaction, and deposition is generated. Table 2 shows the relationship between the annual-average parameters for simplified simulation and the original hourly variables. In InMAP-China, the annual averaged component and the deviation of wind speed to represent advection are calculated using hourly elements. The offset of wind vectors in different directions may result in some uncertainties in this process. The parameters of eddy diffusion and convective transport are precalculated using hourly elements, including temperature, pressure, boundary layer height, etc. The annual wet deposition rate is determined by the rainwater mixing ratio and cloud fractions. The annual dry deposition rate of particles and gaseous pollutants at the surface level is precalculated using friction speed, heat flux, radiation flux and land cover. The simplification of chemical reactions is different among pollutants. For NO_x, NH_3, and volatile organic compound (VOC) precursors, the annual averaged gas-particle partitioning is adopted and calculated before using the output concentrations of species from CMAQ. For SO_2 pollutants, the annual oxidation rate of two major conversion pathways for SO_2 is calculated using concentrations of hydroxyl radical (HO) and hydrogen peroxide (H_2O_2) in CMAQ, and the conversion is estimated in InMAP-China.

2.1.2 Prior WRF-CMAQ simulation

To generate the meteorological and chemical parameters required by InMAP-China, a one-year WRF-CMAQ simulation covering the entire mainland of China is conducted to output hourly meteorological and chemical-related variables in the year 2017. Besides, the nested WRF-CMAQ

simulation over the BTH region is also conducted and validated using observed data. The corresponded output data is used to generate the meteorological and chemical parameters required by InMAP-China for the simulations of 4 km resolution in the BTH region. Tables S1 and S2 show the major configurations of the WRF-CMAQ modelling system. The WRF model is driven by the National Centers for Environmental Prediction Final Analysis (NCEP-FNL) (https://doi.org/10.5065/D6M043C6) reanalysis data to provide the initial and boundary conditions. The meteorological fields derived from the WRF model is used to drive the CMAQ model (Appel et al., 2016) simulations. The air pollutant emissions used here include anthropogenic emissions over China derived from the MEIC model (http://meicmodel.org/), anthropogenic emissions over the region of East Asia outside China derived from the MIX-2010 inventory (Li et al., 2015), and biogenic emissions derived from the MEGANv2.10 model. The CB05 chemical mechanism and the AERO6 aerosol module are employed in the model simulation.

Table S3 summarizes the performance statistics of meteorological variables, including surface temperature, relative humidity, and wind speed, in China in 2017, as simulated by the WRF model. The hourly observed data of major meteorological variables derived from the National Climate Data Center (NCDC) are utilized here. The results show that the meteorological variables simulated by the WRF model agree well with the surface observations, which is consistent with previous studies (Wu et al., 2019; Zheng et al., 2015; Hong et al., 2017). The model performs well on the predictions of surface temperature, with an MB of -0.7 K, an NMB of -6.1%, and R of 0.9. The predictions of relative humidity at a height of 2 metres are relatively satisfied with an MB of 4.1% and an NMB of 6.1%. The predictions of wind speed at a height of 10 metres are slightly overestimated, with an MB of 0.3 m/s and an NMB of 12.4%, which may be caused by out-of-date USGS land use data employed in the model runs.

The SO_2, NO_2 and $PM_{2.5}$ concentrations modelled across the domain agree well with the surface observations in terms of the statistical performance and monthly variations. Table S4 summarizes the performance of the statistics of major air pollutant concentrations. The nationwide annual averaged $PM_{2.5}$ concentration simulated in 2017 in China was 42.1 $\mu g/m^3$. Compared with the observed $PM_{2.5}$ of 45.9 $\mu g/m^3$, there are slight underpredictions with an MB of 3.7 $\mu g/m^3$ and NMB of 8.1%. The CMAQ model has moderate underpredictions of the NO_2 concentrations and SO_2 concentrations, which may be related to the uncertainties of emission inputs. For modelled NO_2 concentrations, MB and NMB are -4.6 $\mu g/m^3$ and -13.9%, respectively. For modelled SO_2 concentrations, MB and NMB are -0.8 $\mu g/m^3$ and -4.5%,

respectively. Figure S3 shows the monthly variation. The variation trend of the observed SO_2, NO_2, and $PM_{2.5}$ concentrations can basically be reproduced in the CMAQ simulations.

2.1.3 Preprocessed emission input data

We develop the preprocessed module to generate vector emission input for the InMAP-China simulation. This module can allocate air pollutant emissions vertically and horizontally to supply the missing parameters for the emission file and convert them into a shapefile vector format. The shapefile vector format's emission data of 36km resolution in entire mainland of China and 4km resolution in the BTH region in 2017 are pre-processed by using this module.

In this module, the emission data are preprocessed by source and altitude. The anthropogenic emissions of five sectors in China in 2017 from the MEIC inventory (http://meicmodel.org/), the anthropogenic emissions over regions outside mainland China in Asia from the MIX-2010 inventory (Li et al., 2015), and the natural emissions estimated using the MEGANv2.10 model (Guenther et al., 2012) are employed in this study.

More detailed, the gridded anthropogenic emissions of 0.3 degrees for the residential, transportation, and agricultural sectors are preprocessed and input to the surface layer. The gridded air pollutant emissions of the industrial sector and noncoal power plants are preprocessed for allocation to attitudes ranging from 130 metres to 240 metres and 130 metres to 890 metres, respectively. The emissions of coal-fired power plants (CPPs) are preprocessed as point sources. The air pollutant emissions and the stack attribution of each unit are provided in the emission file. Because the stack attribution of the power unit is missed in the MEIC inventory, we supplied the information in the preprocessed module based on NEI (National Emission Inventory data) data of power units. For stack height/stack diameter, a linear relationship is first established (see Figure S1), and then, supplementation for these two parameters of Chinese power plants is conducted by using the relationships. The fixed value for the other two variables of stack attribution is set here because the $PM_{2.5}$ concentrations attributable to power plants (CPPs-$PM_{2.5}$) are less sensitive to the two variables (see Figure S2). The stack gas exit velocity and stack gas exit temperature of the power unit are 6 m/s and 313 K, respectively. The air pollutant emissions over regions outside mainland China in Asia and the natural emissions simulated by MEGANv2.10 are preprocessed and input to the surface layer.

208 **2.1.4 Exposure-response function from GEMM**

209 To rapidly estimate the premature mortality of $PM_{2.5}$ exposures, we employ the exposure-response
210 function from GEMM to estimate $PM_{2.5}$-related premature mortality, which was developed by Burnett
211 et al. (Burnett et al., 2018), and calculate the premature mortality using $PM_{2.5}$ concentration predictions
212 of InMAP-China. Premature mortality due to non-communicable diseases (NCDs) and lower respiratory
213 infections (LRIs) was considered in this study. Mortality is determined by the mortality incidence rate,
214 population, and attributable fraction (AF) to certain $PM_{2.5}$ concentrations. The national mortality
215 incidence rate and the population data were derived from the GBD2017 study (Institute for Health
216 Metrics and Evaluation). The spatial distribution of the population in 2015 from the Gridded Population
217 of World Version 4 (Doxsey et al., 2015) was employed to allocate the population in 2017.

218 **2.2 Evaluation protocol**

219 **2.2.1 Evaluation method**

220 In this study, the performances of the InMAP-China predictions are evaluated by comparison
221 against CMAQ simulations and surface observations. Model-to-model comparison and model-to-
222 observation comparison have both been used to evaluate the performance of reduced-complexity air
223 quality models in previous studies (Tessum et al., 2017, Gilmore et al., 2019).

224 The following aspects are considered to make an evaluation. First, we examine the ability of
225 InMAP-China to predict $PM_{2.5}$ concentrations at different emission levels, which will be introduced in
226 Section 3.1. Second, to examine the ability to quantify source contributions to $PM_{2.5}$ concentrations, we
227 compare the InMAP-China's predictions of the sectoral contributions attributable to power, industry,
228 residential, transportation, and agriculture with those based on the CMAQ model, which will be
229 presented in Section 3.2. Third, to comprehensively understand the performance at higher spatial
230 resolution using InMAP-China, we compare the predictions of $PM_{2.5}$ concentrations at 4km spatial
231 resolution in the BTH region both modelled by InMAP-China and conventional CMAQ with the
232 observations, which is displayed in Section 3.3. Fourth, focusing on the health impacts, the $PM_{2.5}$-related
233 premature mortality predicted by InMAP-China is also compared with mortality estimation based on
234 $PM_{2.5}$ exposure derived from CMAQ, which is presented in Section 3.4.

235 For the observed $PM_{2.5}$ concentration data, the annual averaged observed $PM_{2.5}$ concentrations in
236 2017 were calculated using hourly concentration data from the China National Environmental
237 Monitoring Center, CNEMC (http://www.cnemc.cn/). More than 1400 national monitoring sites for air

pollutant concentrations are included in the simulation domain. The statistical parameters used in this study include the correlation coefficient (R), mean bias (MB), mean error (ME), normalized mean bias (NMB), normalized mean error (NME), and root mean square error (RMSE). The statistical analyses on the performance of InMAP-China are similar to our previous evaluation of conventional CTMs (Zheng et al., 2015; Wu et al., 2019).

2.2.2 Experimental design

We design twelve simulations to examine the model ability of InMAP-China in this study. Table 3 shows the sequence of simulations.

InMAP_TOT represents the baseline simulation with maximum emissions input, in which five sectoral anthropogenic emissions are derived from the MEIC inventory, natural emissions are derived from the MEGANv2.10 model, and Asian emissions outside mainland China are derived from the MIX-2010 inventory are combined as emission inputs. Five sectoral and five abatement simulations are also conducted to examine the ability of InMAP-China to predict concentration changes in response to sectoral emissions and abatement emissions. The emission inputs for these ten simulations have been declared in Table 3. The annual averaged physical and chemical process parameters are calculated based on the output variables of WRF-CMAQ model, which has already been mentioned in Section 2.1.2. Based on the above input, the particle continuity equations are solved by InMAP-China model to obtain the annual averaged $PM_{2.5}$ concentrations at the steady-state of the atmosphere. The above simulations are all conducted at 36km spatial resolution across the entire mainland of China. Besides, another simulation represented by InMAP-BTH is conducted at 4km spatial resolution over the BTH region, with the anthropogenic emission input data at 4km resolution derived from the MEIC inventory and natural emissions derived from the MEGANv2.10 model is utilized in this simulation.

In order to make a comparison with the InMAP-China simulations, eleven CMAQ simulations are also performed under the same emission inputs. The hourly $PM_{2.5}$ concentrations simulated by CMAQ in 2017 are averaged at obtain the annual averaged $PM_{2.5}$ concentrations. Due to limited computational resources, each simulation is conducted for four representative months (January, April, July, and October) in 2017.

3 Results and Discussion

3.1 Model performance of $PM_{2.5}$ concentrations in China

3.1.1 Total $PM_{2.5}$ concentrations

Figure 3 shows the performance evaluation of total $PM_{2.5}$ concentrations in the InMAP_TOT simulations. Compared with the observed annual averaged $PM_{2.5}$ concentrations, the total $PM_{2.5}$ concentrations are moderately underpredicted by InMAP-China with an MB of -8.1 $\mu g/m^3$ and an NMB of -18.1%. Compared with the CMAQ predictions, the total $PM_{2.5}$ concentrations are also underpredicted, with an MB of -5.3 $\mu g/m^3$ due to the underprediction of primary $PM_{2.5}$. Consistent air pollutant emissions are employed in the CMAQ and InMAP-China simulations. Therefore, the underpredictions are caused by the different mechanisms in the two models. Basically, InMAP-China reproduces the spatial pattern of total $PM_{2.5}$ concentrations simulated by CMAQ. Notably, significant overpredictions of $PM_{2.5}$ concentrations can be observed over mountain areas across Northern China, and the complex terrain and large emission intensity increase the challenge of predicting $PM_{2.5}$ concentrations using the reduced-complexity air quality model in this region.

Figure 4 shows a comparison of $PM_{2.5}$ compositions. Compared with the CMAQ results, the InMAP-China predictions of $PM_{2.5}$ compositions are satisfactory, with NMBs for SO_4^{2-}, NO_3^-, NH_4^+, and primary $PM_{2.5}$ equal to 13%, -8%, -10%, and -23%, respectively. The predictions of SO_4^{2-}, NO_3^-, and NH_4^+ perform better than those of primary $PM_{2.5}$. Figure 5 and Figure 6 compare the spatial distribution of $PM_{2.5}$ compositions, and similar over-predictions of $PM_{2.5}$ compositions can be observed in the mountain area in Northern China.

The ability of InMAP-China to predict $PM_{2.5}$ compositions is also examined at various emission levels. Figure 7 compares the concentrations of $PM_{2.5}$ compositions and the proportions of secondary inorganic aerosols (hereafter, SNA) in total $PM_{2.5}$ concentrations in different scenarios by two models. In the InMAP_TOT scenario, the proportion of SNA is 56%, which is extremely close to the 50% proportion in the WRF-CMAQ simulations. In five emission abatement simulations, the proportion was approximately equal to that in the baseline scenario because the linearly treated chemical reaction relationship of SNA was employed in InMAP-China. However, focusing on the simulations of five sectoral emission scenarios, a significant difference can be observed, which is mainly caused by the difference in chemical treatments in InMAP-China and CMAQ. In this situation, the impacts on $PM_{2.5}$ concentrations are distinct due to the nonlinear emission-concentration process.

3.1.2 Marginal change in $PM_{2.5}$ concentrations

Figure 8 compares the InMAP-China and CMAQ predictions of population-weighted $PM_{2.5}$ concentrations and $PM_{2.5}$ compositions for eleven emission scenarios. Marginal changes in air pollutant concentrations are defined as 1 $\mu g/m^3$ by normalizing the population-weighted air pollutant concentrations of each scenario using the largest value among all scenarios modelled by CMAQ. The InMAP-China reproduces CMAQ predictions on the marginal change in population-weighted $PM_{2.5}$ concentrations, with a NMB of -12% and correlations of 0.98, as shown in Figure 8(a). This performance is similar to that predicted by InMAP in the United States (Tessum et al., 2017).

Figure 8(b)-(f) compares the predictions of $PM_{2.5}$ compositions. The InMAP-China predictions of SO_4^{2-}, NO_3^-, NH_4^+ and primary $PM_{2.5}$ agree well with the CMAQ results, but the predictions of secondary organic aerosol (SOA) are the poorest. The marginal changes in NO_3^- and primary $PM_{2.5}$ concentrations are moderately underpredicted by InMAP-China, with NMB values of -13% and -21%, respectively. Conversely, the marginal change in SO_4^{2-} concentrations is overpredicted with an NMB of 23%. The marginal change in NH_4^+ predicted by InMAP-China agrees well with the CMAQ predictions. Because few reaction pathways of SOA are included in the CB05 mechanism in the CMAQ simulations, SOAs are underpredicted in the entire modelling system.

The regional performance of the changes in $PM_{2.5}$ and its compositions for eleven emission scenarios is also examined in this study. Figures S4-S7 show the regional results. Four regions, including the Beijing-Tianjin-Hebei region (BTH), Yangtze River Delta (YRD), Pearl River Delta (PRD), and Fen Wei Plain (FWP), are analysed here (see Figure 2). At the regional level, the CMAQ predicted marginal changes in population-weighted $PM_{2.5}$ concentrations, and its composition can be reproduced by InMAP-China, which is similar to the nationwide performance. However, the marginal change in SO_4^{2-} concentrations over the BTH is significantly overpredicted by InMAP-China, with an NMB of 135%, which is expected to be improved by optimizing the representation of the annual sulfate oxidation rate in this region.

3.2 Model performance of source contributions in China

Figure 9 shows the contribution of each sector to $PM_{2.5}$ concentrations nationwide and at the regional scale, and Table 4 displays the proportion value of sectoral contribution based on two models. The predictions of the source contributions of $PM_{2.5}$ concentrations in InMAP-China are basically reliable compared with those based on the CMAQ model, and the difference can be explained.

The results based on the two models indicate that the industrial and residential sectors are the first and second contributors among the five sectors. The contribution of the electricity sector is comparable when using the two models, while the contributions of transportation and agriculture are moderately different, which is mainly due to the difference in the model mechanism and the treatment of secondary inorganic aerosols in the two models. At the regional scale, the difference in the sectoral contribution caused by the mechanism in the two models is more significant than at the national scale.

3.3 Model performance of $PM_{2.5}$ predictions at higher resolution in the BTH region

We also conducted a simulation with higher spatial resolution of 4 km in the BTH region by using InMAP-China model and make a comparison with the WRF-CMAQ nested simulation at the same area in the BTH region. Figure 10 and Figure 11 show the performance evaluation of total $PM_{2.5}$ concentration and the composition in the InMAP_BTH scenario. Compared with the observed annual averaged $PM_{2.5}$ concentrations, the total $PM_{2.5}$ concentrations are moderately overpredicted in InMAP_BTH with an NMB of 41.3% and an R of 0.5.

Further compared with the nested CMAQ predictions, the total $PM_{2.5}$ concentrations are also over-predicted by InMAP-China model. The predictions of $PM_{2.5}$ compositions in the InMAP_BTH scenario are partially satisfactory, except for SO_4^{2-}, with NMBs for SO_4^{2-}, NO_3^-, NH_4^+, and primary $PM_{2.5}$ equal to 178%, 36%, 33%, and 27%, respectively. Figure 12 further shows the comparison of the spatial distribution of $PM_{2.5}$ compositions in the BTH region. The overall spatial distribution pattern of $PM_{2.5}$ compositions is similarly modeled by two models, however, an obvious difference can be observed across the mountain area in the BTH region, for instance, the over-predictions of $PM_{2.5}$ compositions, especially, SO_4^{2-} and NO_3^- observed near the Taihang mountain area.

3.4 Model performance of $PM_{2.5}$-related premature mortality in China

To examine the performance of the predictions of $PM_{2.5}$-related premature mortality, a comparison of premature mortality using the $PM_{2.5}$ predictions from InMAP-China and CMAQ, separately, is performed here. Figure 13 shows the comparison based on two models for all provinces. The results demonstrate that, compared with the premature mortality based on CMAQ, the relative difference is ranging from -44% to 15% at the provincial level due to the difference of $PM_{2.5}$ concentrations in the two models.

At the provincial level, the $PM_{2.5}$-related premature mortality in Beijing city, Tianjin city, Hebei province, and Shanghai city is slightly over-predicted by InMAP-China, with the relative difference

ranging from 4% to 15%. Conversely, for the other majority of provinces, $PM_{2.5}$-related premature mortality is under-predicted by InMAP-China, with the relative difference ranging from -3% to -44%. Overall, the $PM_{2.5}$-related premature mortality estimated using InMAP-China was 1.92 million people in 2017. Compared with the CMAQ-based estimations, 25 ten thousand deaths are under-predicted by InMAP-China because of underestimation of total $PM_{2.5}$ concentrations in the baseline simulation.

4 Conclusions

This work develops a reduced-complexity air quality intervention model over China and presents a comprehensive evaluation by comparing CMAQ simulations and surface observations. The InMAP-China aims at providing a simplified modeling tool to rapidly predict the $PM_{2.5}$ concentrations due to emission change as well as health impact of emission sources in China. After the model is established, the total consumed time for a new simulation under the atmosphere condition in the year 2017 across the mainland of China using InMAP-China is merely an hour with a single CPU of 24 nodes. Therefore, it is time-efficient when conduct new simulations of $PM_{2.5}$ concentrations in China. Notably, the running of WRF-CMAQ simulations is merely necessary in our developing stage of InMAP-China. For the application of InMAP-China, we recommend users to select InMAP-China as a prior tool with extensive simulation demands, for instance, to quantify the $PM_{2.5}$ concentrations due to hundreds of pollution emitters or to rapidly estimate the $PM_{2.5}$ concentrations caused by dozens of control policies, separately. Besides, the variable grid can also be set in InMAP-China to allow high spatial resolution of 1km or even higher in certain urban area.

InMAP-China has moderately satisfactory performance in this study, however, this model has reductions in accuracy compared with conventional CTMs. Overall, InMAP-China satisfactorily predicts total $PM_{2.5}$ concentrations in the baseline simulation in terms of statistical performance. Compared with the observed $PM_{2.5}$ concentrations, the MB, NMB, and correlations of the total $PM_{2.5}$ concentrations are -8.1 $\mu g/m^3$, -18%, and 0.6, respectively. The statistical performance is satisfactory for a reduced-complexity air quality model and remains consistent with the performance evaluation in the United States. The underestimation of total $PM_{2.5}$ mainly comes from the primary $PM_{2.5}$. Moreover, the spatial pattern of total $PM_{2.5}$ concentrations can be reproduced in InMAP-China, while an overestimation over the mountain area in Northern China can be observed. The large emission intensity and complex terrain over this region increase the difficulty of modelling concentrations in this area. The predictions of source contributions to $PM_{2.5}$ concentrations by InMAP-China are comparable with those based on the CMAQ

model, and the difference is mainly caused by the uncertainty of the simplification of chemical process in the InMAP-China. The global version of reduced-complexity air quality model (Global-InMAP) is also developed and preprint recently (Thakrar et al., 2021), our results of InMAP-China can provide more accurate result in the mainland of China.

This study is subject to some limitations and uncertainties. In InMAP-China, the annual-average chemical and physical processes parameters are calculated using hourly parameters from WRF-CMAQ. Complicated seasonal and daily variations affecting the formation and transportation of particulate matter are challenging to retain. The intensity of advection of the air mass is supposed to be weakened due to the offset of the wind vector in the averaging process, which was also pointed out in a previous study. Moreover, InMAP-China has difficulty predicting SOA concentrations because reaction pathways for SOA are insufficient in this modelling system. Further research work is suggested to improve the model performance. For instance, the combination of machine learning with the simplified simulation may need to research to promote the reduced-complexity air quality modeling over China.

Code and data availability

The source code for the localized version of reduced-complexity air quality model over China (InMAP-China), which is developed based on the original InMAP model over the United states. The data related to this study as well as the user manual are available at https://doi.org/10.5281/zenodo.5111961.

Author contributions

RL. Wu and Q. Zhang designed the research and RL. Wu carried them out. RL. Wu, CW. Tessum and Y. Zhang contributed to model development. RL. Wu prepared the manuscript with contributions from all co-authors.

Competing interests

The authors declare no competing interests.

Acknowledgements

This work was supported by the National Natural Science Foundation of China (41921005 and 41625020). And this work was also funded under Assistance Agreement No. RD835871 awarded by the U.S. EPA to Yale University. The views expressed in this manuscript are those of the authors alone and do not necessarily reflect the views and policies of the U.S. EPA. The EPA does not endorse any products or commercial services mentioned in this publication.

References

A. Xiu, J. E. Pleim. Development of a Land Surface Model. Part I: Application in a Mesoscale Meteorological Model. Journal of Applied Meteorology, 40:192-209, 2011.

Appel, K.W., Napelenok, S.L., Hogrefe, C., Foley, K.M., Pouliot, G.A., Murphy, B., Heath, N., Roselle, S., Pleim, J., Bash, J.O., Pye, H.O.T., Mathur, R. Overview and evaluation of the Community Multiscale Air Quality (CMAQ) modelling system version 5.2. Air Pollution Modelling and its Application XXV, 11:63-72. ITM 2016. Springer Proceedings in Complexity. Springer, Cham, doi: 10.1007/978-3-319-57645-9_11, 2017.

Appel, K.W., Napelenok, S.L., Hogrefe, C., Foley, K.M., Pouliot, G.A., Murphy, B., Heath, N., Roselle, S., Pleim, J., Bash, J.O., Pye, H.O.T., Mathur, R. Overview and evaluation of the Community Multiscale Air Quality (CMAQ) modelling system version 5.2. Air Pollution Modelling and its Application XXV, 11:63-72. ITM 2016. Springer Proceedings in Complexity. Springer, Cham, doi: 10.1007/978-3-319-57645-9_11, 2017.

Baker, K. R.; Amend, M.; Penn, S.; Bankert, J.; Simon, H.; Chan, E.; Fann, N.; Zawacki, M.; Davidson, K.; Roman, H., A database for evaluating the InMAP, APEEP, and EASIUR reduced complexity air-quality modelling tools. Data in Brief, 28, 2020.

Burnett, R.; Chen, H.; Szyszkowicz, M.; Fann, N.; Hubbell, B.; Pope, C. A.; Apte, J. S.; Brauer, M.; Cohen, A.; Weichenthal, S.; Coggins, J.; Di, Q.; Brunekreef, B.; Frostad, J.; Lim, S. S.; Kan, H. D.; Walker, K. D.; Thurston, G. D.; Hayes, R. B.; Lim, C. C.; Turner, M. C.; Jerrett, M.; Krewski, D.; Gapstur, S. M.; Diver, W. R.; Ostro, B.; Goldberg, D.; Crouse, D. L.; Martin, R. V.; Peters, P.; Pinault, L.; Tjepkema, M.; Donkelaar, A.; Villeneuve, P. J.; Miller, A. B.; Yin, P.; Zhou, M. G.; Wang, L. J.; Janssen, N. A. H.; Marra, M.; Atkinson, R. W.; Tsang, H.; Thach, Q.; Cannon, J. B.; Allen, R. T.; Hart, J. E.; Laden, F.; Cesaroni, G.; Forastiere, F.; Weinmayr, G.; Jaensch, A.; Nagel, G.; Concin, H.; Spadaro, J. V., Global estimates of mortality associated with long-term exposure to outdoor fine particulate matter. Proceedings of the National Academy of Sciences of the United States of America, 115, (38), 9592-9597, 2018.

C. J. Walcek, Taylor GR. A Theoretical Method for Computing Vertical Distributions of Acidity and Sulfate Production within Cumulus Clouds. Journal of the Atmospheric Science, 43:339-55, 1986.

Chang, X.; Wang, S.; Zhao, B.; Xing, J.; Liu, X.; Wei, L.; Song, Y.; Wu, W.; Cai, S.; Zheng, H.; Ding, D.; Zheng, M., Contributions of inter-city and regional transport to $PM_{2.5}$ concentrations in the Beijing-Tianjin-Hebei region and its implications on regional joint air pollution control. Science of the Total Environment, 660, 1191-1200, 2019.

Cohen, A. J.; Brauer, M.; Burnett, R.; Anderson, H. R.; Frostad, J.; Estep, K.; Balakrishnan, K.; Brunekreef, B.; Dandona, L.; Dandona, R.; Feigin, V.; Freedman, G.; Hubbell, B.; Jobling, A.; Kan, H.; Knibbs, L.; Liu, Y.; Martin, R.; Morawska, L.; Pope, C. A., III; Shin, H.; Straif, K.; Shaddick, G.; Thomas, M.; van Dingenen, R.; van Donkelaar, A.; Vos, T.; Murray, C. J. L.; Forouzanfar, M. H., Estimates and 25-year trends of the global burden of disease attributable to ambient air pollution: an analysis of data from the Global Burden of Diseases Study 2015. Lancet 389, (10082), 1907-1918, 2017.

Dimanchevi, E. G.; Paltsev, S.; Yuan, M.; Rothenberg, D.; Tessum, C. W.; Marshall, J. D.; Selin, N. E., Health co-benefits of sub-national renewable energy policy in the US. Environmental Research Letters, 14, (8) ,2019.

Doxsey-Whitfield E, MacManus K, Adamo S B, Susana B, Pistolesi L, Squires J, BorkovskaOand Baptista S R Taking advantage of the improved availability of census data: a first look at the gridded population of the world, version 4. Papers in Applied Geography. 1 226–34, 2015.

E. J. Mlawer, S. J. Taubman, P. D. Brown, M. J. Iacono, S. A. Clough. Radiative transfer for inhomogeneous atmospheres: RRTM, a validated correlated-k model for the longwave. Journal of Geophysical Research, 102:16663-82, 1997.

Fountoukis C and Nenes A. ISORROPIA II: A Computationally Efficient Aerosol Thermodynamic Equilibrium Model for K^+, Ca^{2+}, Mg^{2+}, NH_4^+, Na^+, SO_4^{2-}, NO_3^-, Cl^-, H_2O Aerosols, Atmospheric Chemistry Physics, 7, 4639-4659, 2007.

Gilmore, E. A.; Heo, J.; Muller, N. Z.; Tessum, C. W.; Hill, J. D.; Marshall, J. D.; Adams, P. J., An inter-comparison of the social costs of air quality from reduced-complexity models. Environmental Research Letters, 14, (7), 2019.

Global Burden of Disease Collaborative Network. Global Burden of Disease Study 2017 (GBD 2017) Population Estimates 1950-2017. Seattle, United States: Institute for Health Metrics and Evaluation (IHME), 2018.

Global Burden of Disease Collaborative Network. Global Burden of Disease Study 2017 (GBD 2017) Cause-Specific Mortality 1980-2017. Seattle, United States: Institute for Health Metrics and Evaluation (IHME), 2018.

Goodkind AL, Tessum CW, Coggins JS, Hill JD, Marshall JD. Fine-scale damage estimates of particulate matter air pollution reveal opportunities for location-specific mitigation of emissions. Proceedings of the National Academy of Sciences. Apr 3:201816102. https://doi.org/10.1073/pnas.1816102116, 2019.

Guenther, A. B.; Jiang, X.; Heald, C. L.; Sakulyanontvittaya, T.; Duhl, T.; Emmons, L. K.; Wang, X., The Model of Emissions of Gases and Aerosols from Nature version 2.1 (MEGAN2.1): an extended and updated framework for modelling biogenic emissions. Geoscientific Model Development Discussions, *5*, (2), 1503-1560, 2012.

Heo, J.; Adams, P. J.; Gao, H. O., Public health costs accounting of inorganic $PM_{2.5}$ pollution in metropolitan areas of the United States using a risk-based source-receptor model. Environment International, 106, 119-126, 2017.

Heo, J.; Adams, P. J.; Gao, H. O., Reduced-form modelling of public health impacts of inorganic $PM_{2.5}$ and precursor emissions. Atmospheric Environment, 137, 80-89, 2016.

Hong, C.; Zhang, Q.; Zhang, Y.; Tang, Y.; Tong, D.; He, K., Multi-year downscaling application of two-way coupled WRF v3.4 and CMAQ v5.0.2 over east Asia for regional climate and air quality modelling: model evaluation and aerosol direct effects. Geoscientific Model Development, 10, (6), 2447-2470, 2017.

J. E. Pleim. A Combined Local and Nonlocal Closure Model for the Atmospheric Boundary Layer. Part I: Model Description and Testing. Journal of Applied Meteorology and Climatology, 46:1383-95, 2007.

J. S. Chang, R. A. Brost, I. S. A. Isaksen, S. Madronich, P. Middleton, W. R. Stockwell, et al. A three-dimensional Eulerian acid deposition model: Physical concepts and formulation. Journal of Geophysical Research, 92:14681-700, 1987.

J. S. Kain. The Kain–Fritsch Convective Parameterization: An Update. Journal of Applied Meteorology. 2004, 43:170-81.

Li, M.; Zhang, Q.; Kurokawa, J.-i.; Woo, J.-H.; He, K.; Lu, Z.; Ohara, T.; Song, Y.; Streets, D. G.; Carmichael, G. R.; Cheng, Y.; Hong, C.; Huo, H.; Jiang, X.; Kang, S.; Liu, F.; Su, H.; Zheng, B., MIX: a mosaic Asian anthropogenic emission inventory under the international collaboration framework of the

MICS-Asia and HTAP. Atmospheric Chemistry and Physics, 17, (2), 935-963, 2017.

Li, X.; Zhang, Q.; Zhang, Y.; Zheng, B.; Wang, K.; Chen, Y.; Wallington, T. J.; Han, W.; Shen, W.; Zhang, X.; He, K., Source contributions of urban $PM_{2.5}$ in the Beijing-Tianjin-Hebei region: Changes between 2006 and 2013 and relative impacts of emissions and meteorology. Atmospheric Environment, *123*, 229-239, 2015.

Liu, F.; Zhang, Q.; Tong, D.; Zheng, B.; Li, M.; Huo, H.; He, K. B., High-resolution inventory of technologies, activities, and emissions of coal-fired power plants in China from 1990 to 2010. Atmospheric Chemistry and Physics, 15, (23), 13299-13317, 2015.

M..-D. Chou, M. J. Suarez, C.-H. Ho, M. M-H. Yan, K.-T. Lee. Parameterizations for Cloud Overlapping and Shortwave Single-Scattering Properties for Use in General Circulation and Cloud Ensemble Models. Journal of Climate, 11:202-14, 1998.

Muller, N. Z., Mendelsohn, R. Measuring the damages of air pollution in the United States. Journal of Environmental Economics and Management, 54(1), 1–14. https://doi.org/10.1016/j.jeem.2006.12.002,

Muller, N. Z., Mendelsohn, R., & Nordhaus, W. Environmental accounting for pollution in the United States economy. American Economic Review, 101(5), 1649-75. DOI:10.1257/aer.101.5.1649, 2011.

Multi-resolution Emission Inventory of China (http://meicmodel.org/).

National Centers for Environmental Prediction/National Weather Service/NOAA/US Department of Commerce NCEP FNL Operational Model Global Tropospheric Analyses, continuing from July 1999 Dataset (https://doi.org/10.5065/D6M043C6), 2000.

Reddington, C. L.; Conibear, L.; Knote, C.; Silver, B.; Li, Y. J.; Chan, C. K.; Arnold, S. R.; Spracklen, D. V., Exploring the impacts of anthropogenic emission sectors on $PM_{2.5}$ and human health in South and East Asia. Atmospheric Chemistry and Physics, 19, (18), 11887-11910, 2019.

Sergi, B. J.; Adams, P. J.; Muller, N. Z.; Robinson, A. L.; Davis, S. J.; Marshall, J. D.; Azevedo, I. L., Optimizing Emissions Reductions from the U.S. Power Sector for Climate and Health Benefits. Environmental science & technology, 54, (12), 7513-7523, 2020.

Skamarock W, Klemp J, Dudhia J, Gill D, Barker D, Duda M, Huang X,WangWand Powers J A description of the Advanced Research WRF Version 3 NCAR technical note (Boulder, CO: National Center for Atmospheric Research), 2008.

552 Tessum, C. W.; Hill, J. D.; Marshall, J. D., InMAP: A model for air pollution interventions. PLoS One,
553 12, (4), e0176131, 2017.
554 Thakrar S. T.; Tessum C. W.; Apte J. S.;, Balasubramanian S; Millet D. B.; Pandis S. N.; Marshall J. D.;
555 Hill J. D., et al. Global, High-Resolution, Reduced-Complexity Air Quality Modeling Using InMAP
556 (Intervention Model for Air Pollution). Earth, Space and Enviromenta Chemistry (preprinted), 2021.
557 Thind, M. P. S.; Tessum, C. W.; Azevedo, I. L.; Marshall, J. D., Fine Particulate Air Pollution from
558 Electricity Generation in the US: Health Impacts by Race, Income, and Geography. Environmental
559 Science & Technology, 53, (23), 14010-14019, 2019.
560 United States Environmental Protection Agency. National Emission Inventory data.
561 https://www.epa.gov/air-emissions-inventories/2011-national-emissions-inventory-nei-data. 2011.
562 Whitten G Z, Heo G, Kimura Y, et al. A new condensed toluene mechanism for Carbon Bond CB05-TU.
563 Atmospheric Environment, 44(40SI):5346-5355, 2010.
564 Wu, R.; Liu, F.; Tong, D.; Zheng, Y.; Lei, Y.; Hong, C.; Li, M.; Liu, J.; Zheng, B.; Bo, Y.; Chen, X.; Li,
565 X.; Zhang, Q., Air quality and health benefits of China's emission control policies on coal-fired power
566 plants during 2005–2020. Environmental Research Letters, 14, (9), 094016, 2019.
567 Xiao, Q. Y.; Geng, G. N.; Liang, F. C.; Wang, X.; Lv, Z.; Lei, Y.; Huang, X. M.; Zhang, Q.; Liu, Y.; He,
568 K., Changes in spatial patterns of $PM_{2.5}$ pollution in China 2000–2018: Impact of clean air policies.
569 Environment international, 141, 105776, 2020.
570 Zhang, L.; Liu, L. C.; Zhao, Y. H.; Gong, S. L.; Zhang, X. Y.; Henze, D. K.; Capps, S. L.; Fu, T. M.;
571 Zhang, Q.; Wang, Y. X., Source attribution of particulate matter pollution over North China with the
572 adjoint method. Environmental Research Letters, 10, (8), 2015.
573 Zhang, Q.; Zheng, Y.; Tong, D.; Shao, M.; Wang, S.; Zhang, Y.; Xu, X.; Wang, J.; He, H.; Liu, W.; Ding,
574 Y.; Lei, Y.; Li, J.; Wang, Z.; Zhang, X.; Wang, Y.; Cheng, J.; Liu, Y.; Shi, Q.; Yan, L.; Geng, G.; Hong,
575 C.; Li, M.; Liu, F.; Zheng, B.; Cao, J.; Ding, A.; Gao, J.; Fu, Q.; Huo, J.; Liu, B.; Liu, Z.; Yang, F.; He,
576 K.; Hao, J., Drivers of improved $PM_{2.5}$ air quality in China from 2013 to 2017. Proceedings of the
577 National Academy of Sciences of the United States of America, 116, (49), 24463-24469, 2019.
578 Zheng, B.; Zhang, Q.; Zhang, Y.; He, K. B.; Wang, K.; Zheng, G. J.; Duan, F. K.; Ma, Y. L.; Kimoto, T.,
579 Heterogeneous chemistry: a mechanism missing in current models to explain secondary inorganic aerosol

formation during the January 2013 haze episode in North China. Atmospheric Chemistry and Physics, 15, (4), 2031-2049, 2015.

608 **Table 1. Model configurations in InMAP-China.**

Category	Parameters	Configurations
Basic	Research area and period	China, 2017
	Spatial resolution	36 km × 36 km
	Vertical layers	14 layers
	Run type	Steady run
	Variable grid	Static grid
	Projection	Lambert
	Grid numbers	305816
Input	Meteorological and chemical parameters	Calculated using variables from WRFv3.8-CMAQv5.2
	Anthropogenic emissions	MEIC, MIX, MEGAN
	Population data	GPW 2015 and GBD 2017
	Baseline mortality rate	GBD 2017
Output	Air pollutants	$PM_{2.5}$ and its composition concentrations
	Mortality	$PM_{2.5}$-related premature mortality

609

610

611

612

613

614

615

616

617

618

619 **Table 2 The relationship between parameters for simplified simulation and original variables.**

WRF-CMAQ's Variables	Descriptions	InMAP-China's Parameters	Descriptions
U, V, W	Wind fields	UAvg, UDeviation VAvg, VDeviation WAvg, WDeviation	Advection and mixing coefficients
PH, PHB	Base state of geopotential and perturbation geopotential	Dz	Layer heights
PBLH	Planetary boundary layer height	M2d, M2u, Kxxyy, Kzz	Mixing coefficients
T	Potential Temperature	SO_2Oxidation, PlumeHeight	Chemical reaction rates and plume rise
P, PB	Base state pressure plus perturbation pressure		Chemical reaction rates and plume rise
QRAIN	Mixing ratio of rain	ParticleWetdep, GasWetdep	Wet deposition
QCLOUD	Cloud mixing ratio	SO_2Oxidation	Aqueous-phase chemical reaction rates
CLDFRA	Fraction of grid cell covered by clouds	ParticleWetdep, GasWetdep	Wet deposition
SWDOWN,GLW	Downward shortwave and longwave radiative flux at ground level	GasDrydep, ParticleWetdep	Dry deposition
HFX	Surface heat flux	M2d, M2u, Kxxyy, Kzz, Drydep	Mixing and dry deposition
UST	Friction velocity		Mixing and dry deposition
LU_INDEX	Land use type	M2d, M2u, Kxxyy, Kzz	Mixing
DENS	Inverse air density		Mixing and convert between mixing ratio and mass concentration
aVOC	Anthropogenic VOCs that are SOA precursors	aOrgPartitioning	VOCs/SOA partitioning
aSOA	Anthropogenic SOA		
OH, H_2O_2	Hydroxyl radical and hydrogen peroxide concentrations	SO_2Oxidation	Oxidation rates
pNO	ANO_3I, ANO_3J	NOPartitioning	

gNO	NO and NO_2		NO_x partitioning	/pNO_3
pNH	ANH_4I, ANH_4J	NHPartitioning	NH_3/pNH_4 partitioning	
gNH	NH_3			

644 **Table 3 Simulation experiments conducted using InMAP-China.**

Class	Simulations	Emission input	Physical and chemical parameter input
Base	InMAP_TOT	Five sectoral anthropogenic emissions and natural emissions	
High_re	InMAP_BTH	Five sectoral anthropogenic emissions and natural emissions with 4km resolution at BTH region	
Sec1	InMAP_POW	Power plants emissions	
Sec2	InMAP_INDUS	Industrial emissions	
Sec3	InMAP_TRANS	Transportation emissions	
Sec4	InMAP_RESI	Residential emissions	
Sec5	InMAP_AGRI	Agricultural emissions	
Aba1	InMAP_RE10	Reduce the air pollutants emissions by 10% based on InMAP _TOT emissions	Converted using WRF-CMAQv5.2 simulation data in the year of 2017; Remain the same in all simulations.
Aba2	InMAP_RE30	Reduce the air pollutants emissions by 30% based on InMAP _TOT emissions	
Aba3	InMAP_RE50	Reduce the air pollutants emissions by 50% based on InMAP _TOT emissions	
Aba4	InMAP_RE70	Reduce the air pollutants emissions by 70% based on InMAP _TOT emissions	
Aba5	InMAP_RE90	Reduce the air pollutants emissions by 90% based on InMAP _TOT emissions	

645

646

647

648

649

650

651

652

653 **Table 4 Comparison of the proportions of sectoral contributions to $PM_{2.5}$ concentrations using InMAP-**

654 **China and CMAQ.**

Sector	National		BTH		YRD		PRD		FWPY	
	CMAQ	InMAP-China	CMAQ	InMAP-China	CMAQ	InMAP-China	CMAQ	InMAP-China	CMAQ	InMAP-China
Power	6.9%	8.1%	6.2%	9.4%	7.4%	8.6%	10.4%	8.2%	7.0%	10.0%
Industry	30.8%	35.0%	30.2%	38.2%	33.3%	39.1%	37.5%	35.4%	27.7%	31.9%
Residential	25.9%	28.1%	24.7%	28.2%	17.9%	20.8%	19.5%	28.4%	30.0%	33.8%
Transportation	14.0%	17.3%	13.4%	15.6%	15.7%	21.2%	17.1%	17.5%	13.2%	15.0%
Agriculture	22.5%	11.5%	25.5%	10.4%	25.7%	12.4%	15.4%	11.6%	22.0%	9.4%

655

656

657

658

659

660

661

662

663

664

665

666

667

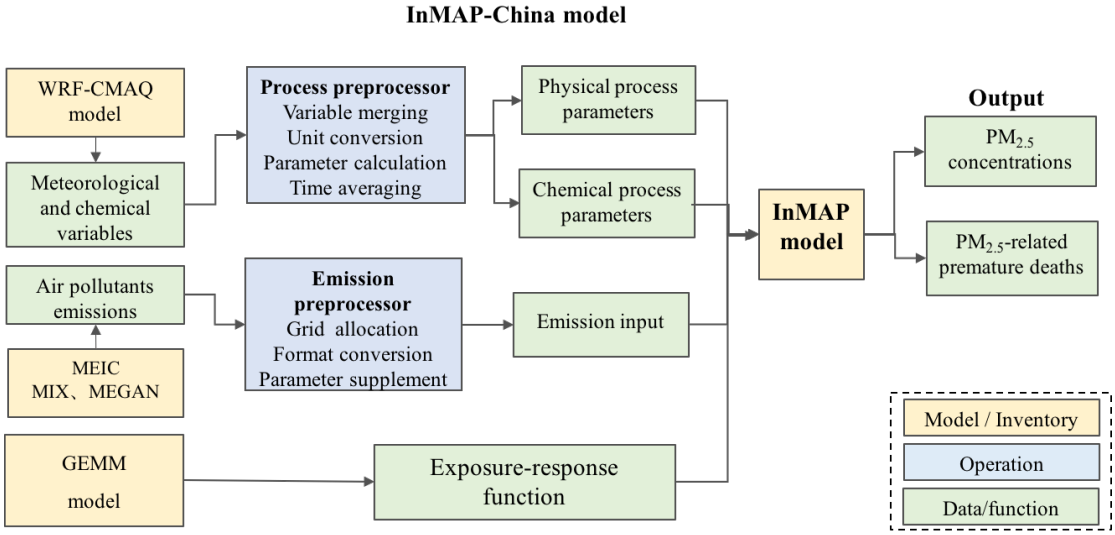

Figure 1 Model framework of InMAP-China.

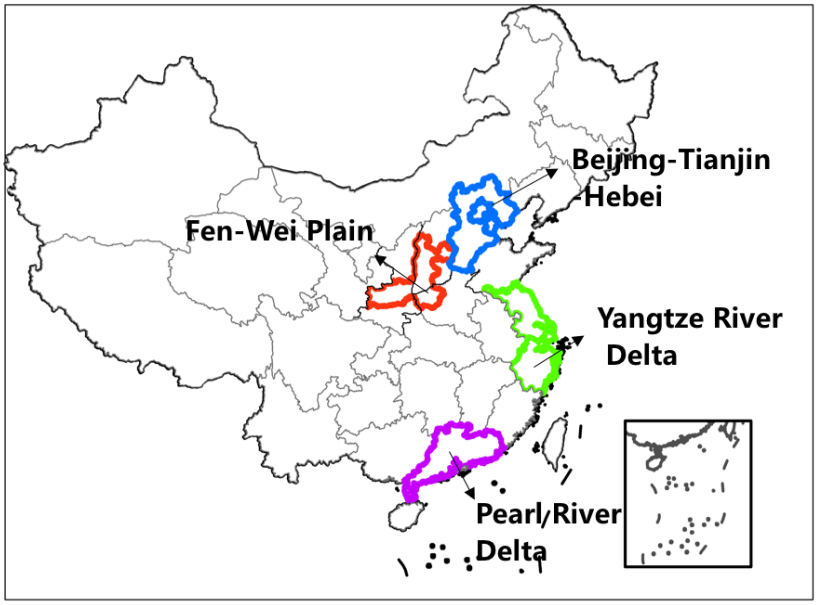

Figure 2 Four key regions defined in this study, including the Beijing-Tianjin-Hebei region, Yangtze River Delta region, Pearl River Delta region and Fen Wei Plain region.

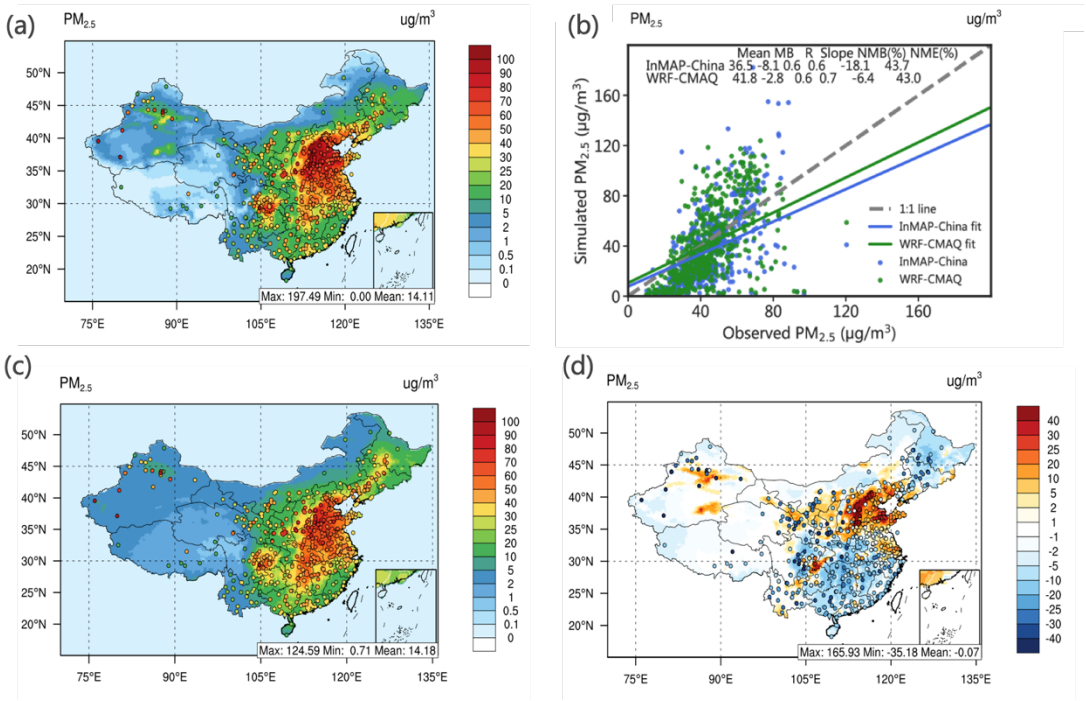

Figure 3 The spatial pattern and statistical metrics of total $PM_{2.5}$ concentrations predicted by InMAP-China and WRF-CMAQ. Panels (a) and (c) display the spatial patterns of total $PM_{2.5}$ concentrations predicted by InMAP-China and WRF-CMAQ, respectively. Panel (d) presents the difference in the spatial distribution of the total $PM_{2.5}$ concentrations predicted by the two models. Panel (b) shows the statistical metrics between the simulated and observed $PM_{2.5}$. The observed total $PM_{2.5}$ concentrations are marked as circles in panel (a) and panel (c). In panel (d), the circle shows the difference between the $PM_{2.5}$ simulated by InMAP-China and the observed $PM_{2.5}$. The same colorbar is utilized in the contour and the marked circle.

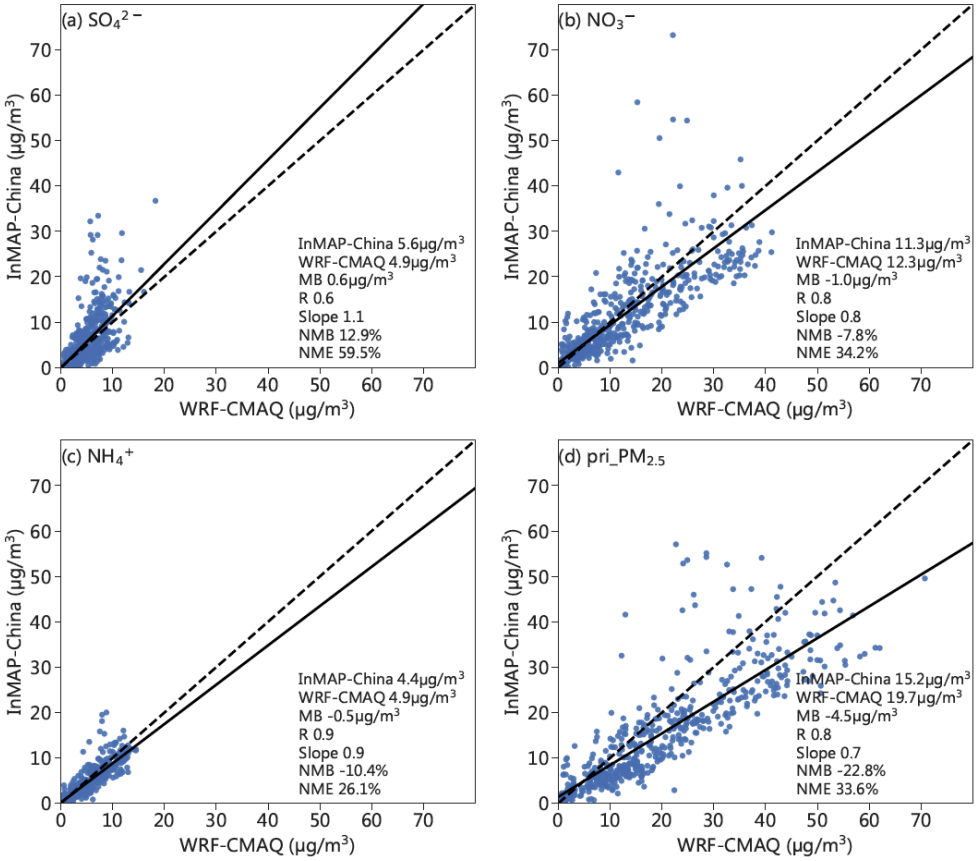

706

707 **Figure 4 Scatter plot comparing the $PM_{2.5}$ composition concentration modelled by the InMAP-China and**

708 **WRF-CMAQ models.** Panels (a), (b), (c) and (d) display sulfate, nitrate, ammonium, and primary $PM_{2.5}$,

709 respectively. The statistical metrics are labelled in the lower right corner of each panel.

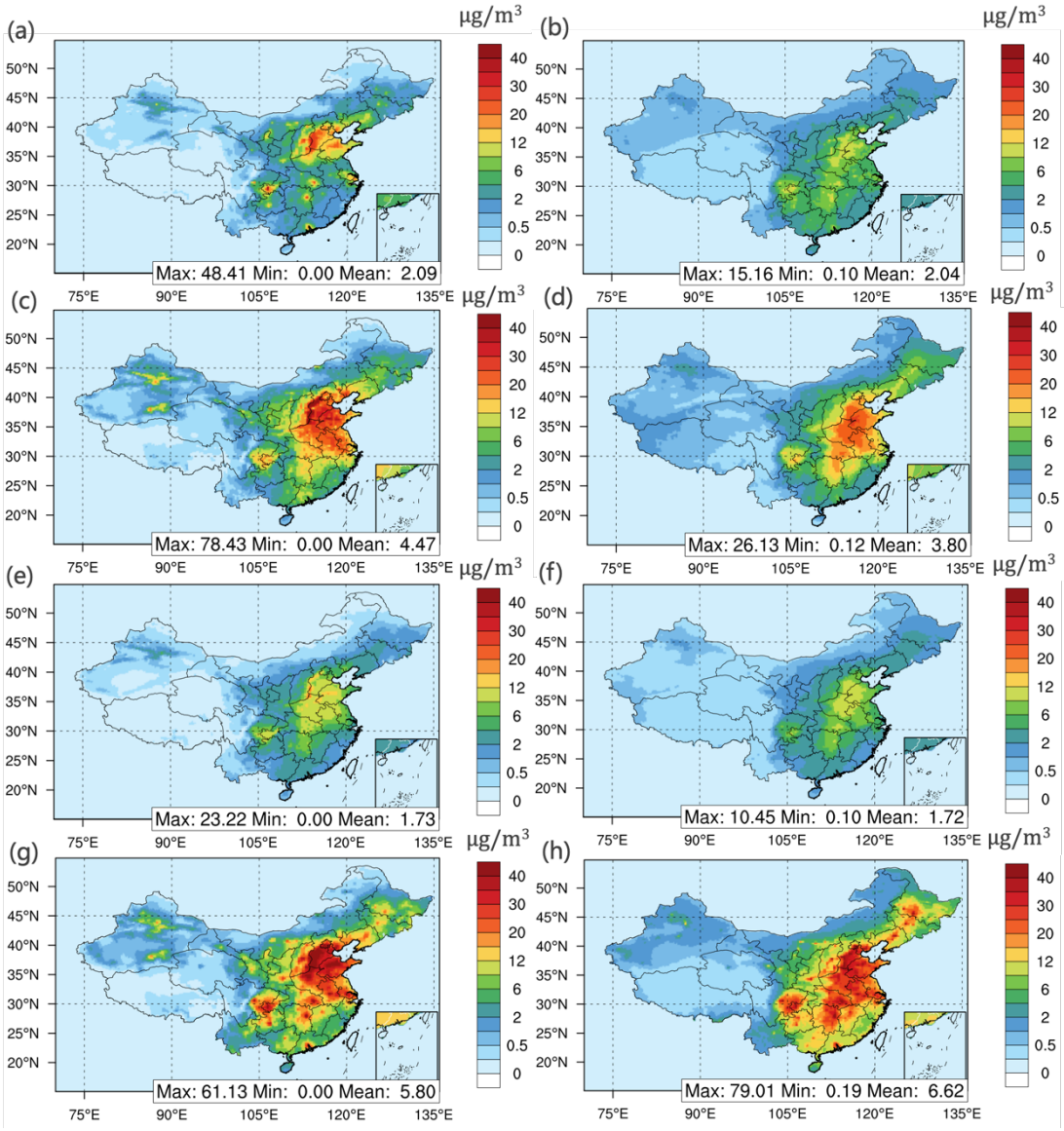

Figure 5 The spatial pattern of $PM_{2.5}$ compositions modelled by the InMAP-China and WRF-CMAQ models. Panels (a), (c), (e), and (g) present the sulfate, nitrate, ammonium, and primary $PM_{2.5}$, respectively, simulated by InMAP-China in the InMAP-TOT scenario. Panels (b), (d), (f), and (h) present the results modelled by WRF-CMAQ.

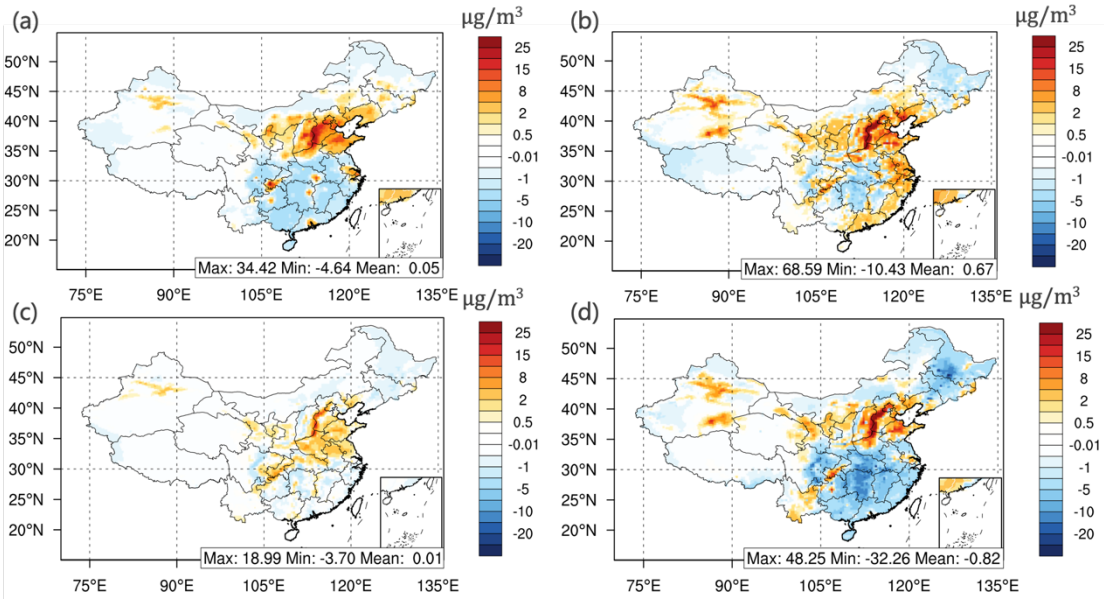

Figure 6 The difference in the spatial pattern of $PM_{2.5}$ compositions between InMAP-China and WRF-CMAQ.

Panels (a), (b), (c), and (d) display sulfate, nitrate, ammonium, and primary $PM_{2.5}$, respectively.

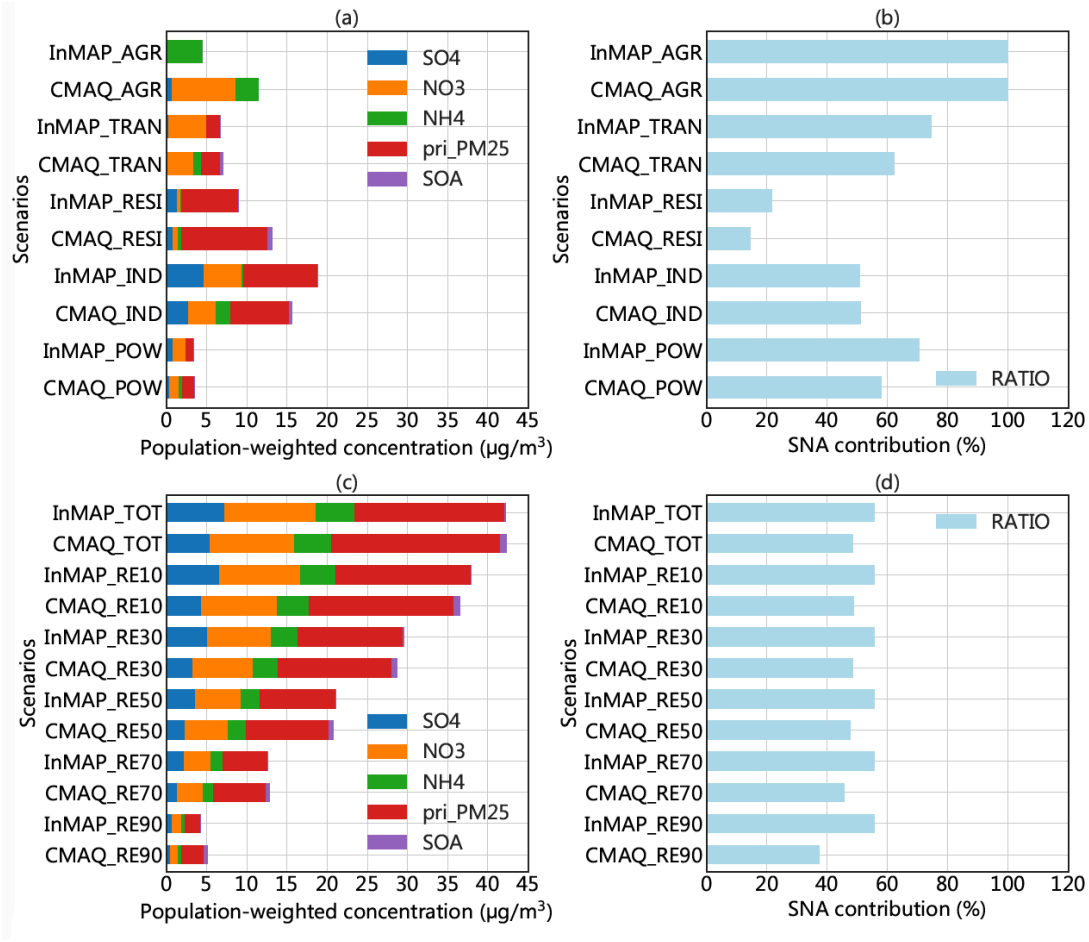

722

723 **Figure 7 Comparison of $PM_{2.5}$ component concentrations and SNA contributions in these eleven simulations.**

724 (a) and (c) show the modelled $PM_{2.5}$ compositions. Panel (a) presents the results of sectoral emission scenarios, and

725 panel (c) presents the results of the baseline and emission abatement scenarios. Panels (b) and (d) present the SNA

726 contribution (%) for each scenario.

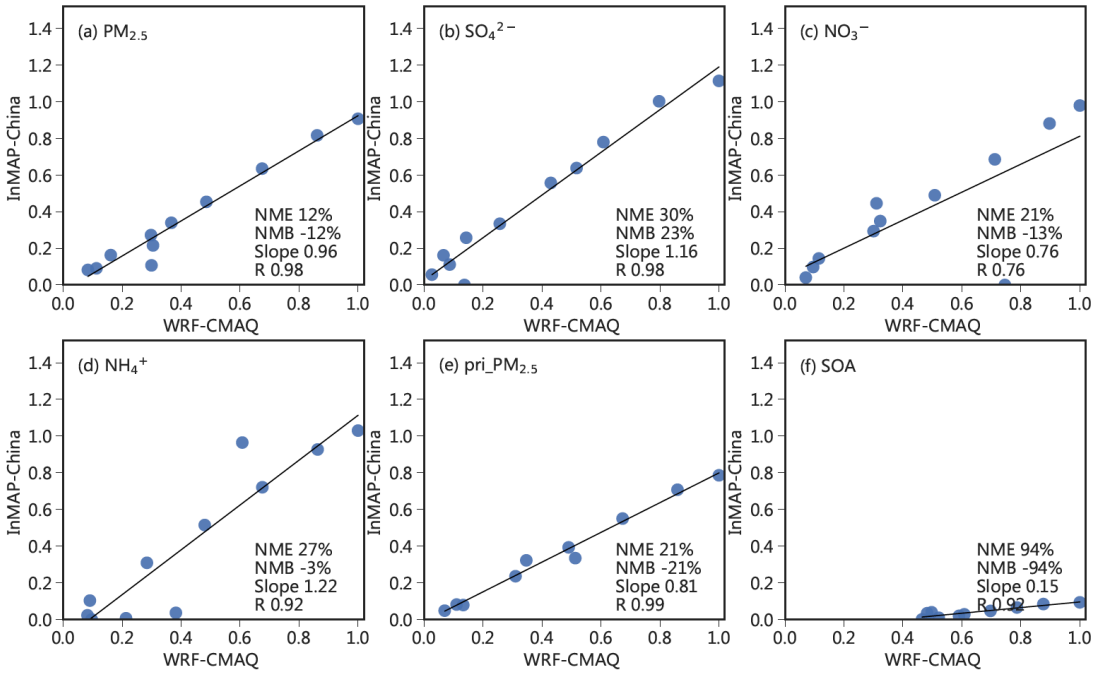

Figure 8 Marginal change in nationwide annual average population-weighted $PM_{2.5}$ concentration and its composition as modelled by InMAP-China and WRF-CMAQ for eleven emissions scenarios. The population-weighted pollutant concentration for each scenario is normalized using the largest value among all scenarios modelled by CMAQ. The eleven dots represent the eleven scenarios, and the statistical metrics are labelled in the lower right corner for each panel.

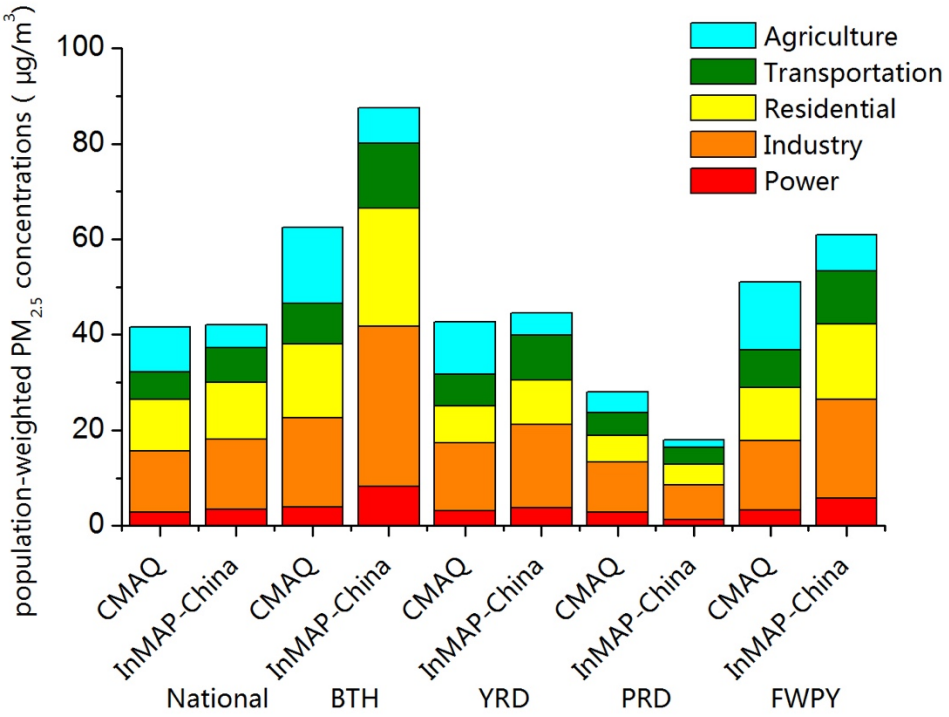

Figure 9 Comparison of source contributions to population-weighted $PM_{2.5}$ concentrations estimated by the two models.

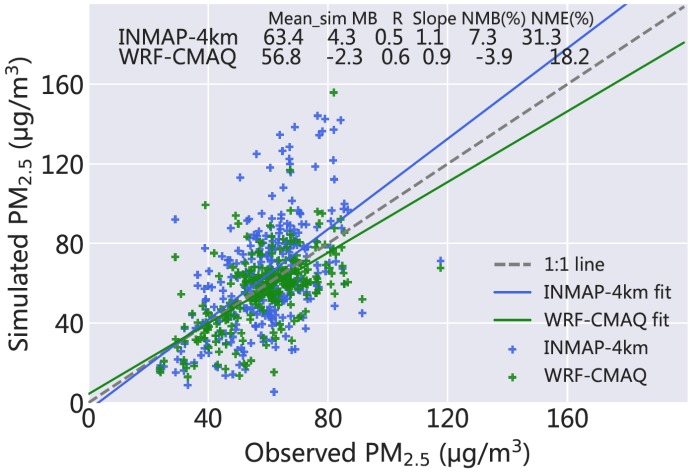

Figure 10 Scatter plot comparing the $PM_{2.5}$ concentration modeled in the BTH region with 4 km spatial resolution by the InMAP-China and WRF-CMAQ. The value of statistical metrics is labeled in the panel.

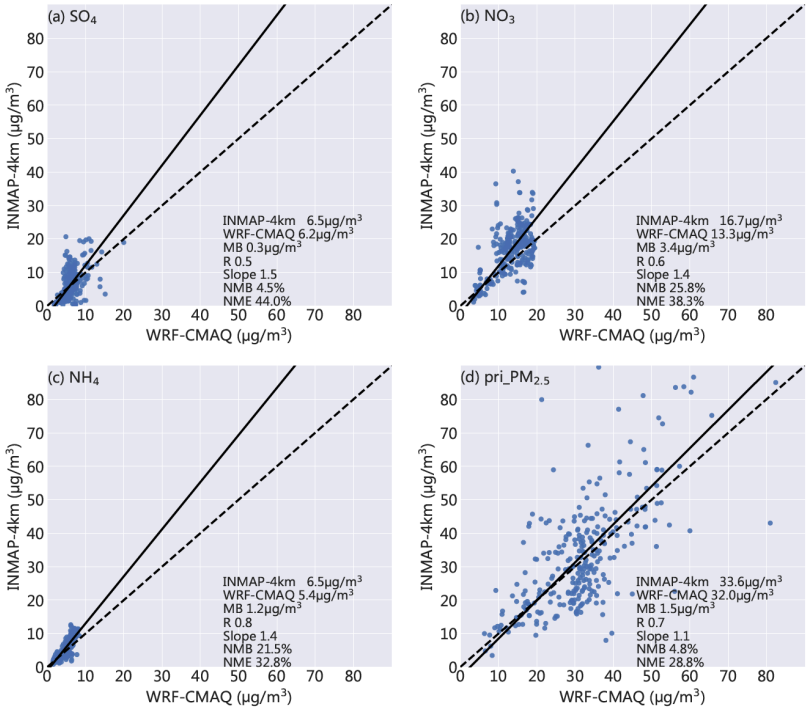

761

762 **Figure 11 Scatter plot comparing the $PM_{2.5}$ composition concentration modeled at BTH region with 4km**

763 **spatial resolution by the InMAP-China and WRF-CMAQ.** Panels (a), (b), (c) and (d) display the sulfate, nitrate,

764 ammonium, and primary $PM_{2.5}$, respectively. The statistical metrics are labeled in the lower right corner of each

765 panel.

766

767

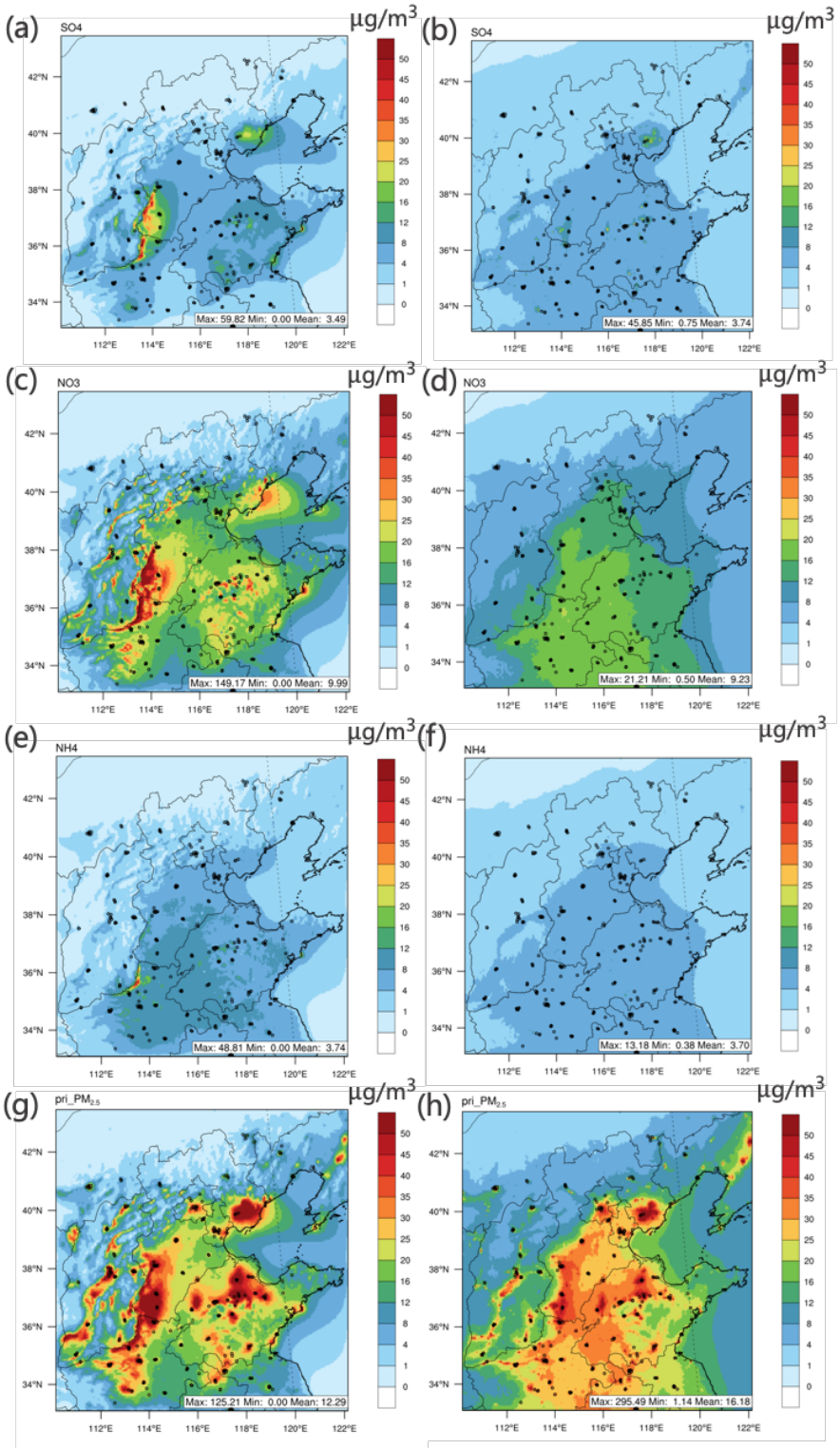

Figure 12 The spatial pattern of $PM_{2.5}$ compositions simulated in the BTH region with 4km spatial resolution by the InMAP-China and WRF-CMAQ. Panels (a), (c), (e), and (g) present the sulfate, nitrate, ammonium, and primary $PM_{2.5}$, respectively, simulated by InMAP-China. Panels (b), (d), (f), and (h) present the corresponding results simulated by WRF-CMAQ.

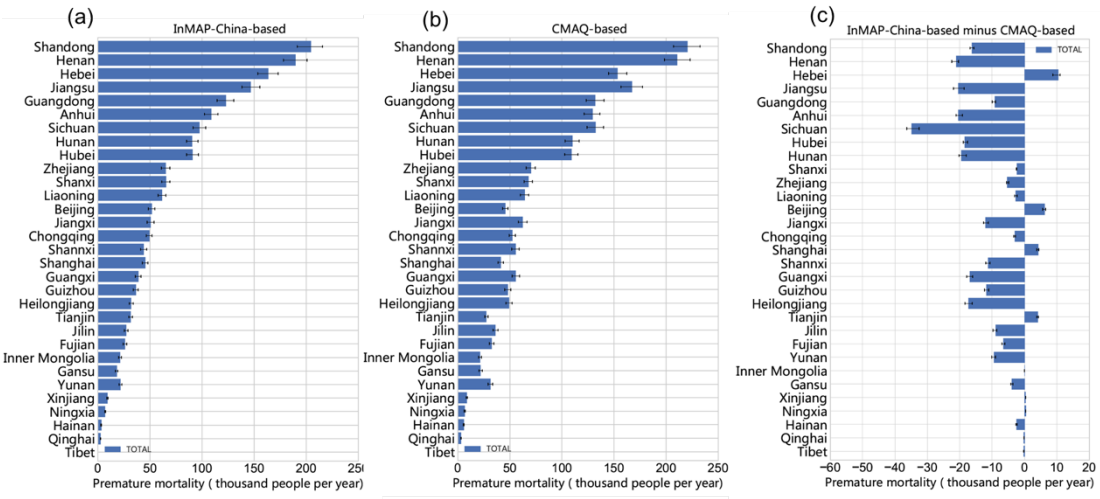

773

774 **Figure 13 Comparison of $PM_{2.5}$-related premature mortality using the $PM_{2.5}$ predictions from two models.**

775 (a) InMAP-China-based; (b) CMAQ-based; and (c) difference between the two models.

776

777

778

779

780

781

782

783

784